

# Influence of Explicit Ions on Titration Curves and Conformations of Flexible Polyelectrolytes: A Monte Carlo Study

Fabrice Carnal, Serge Ulrich, and Serge Stoll\*

*University of Geneva, F.-A. Forel Institute, Group of Environmental Physical Chemistry, 10 Route de Suisse, 1290 Versoix, Switzerland*

*Received August 28, 2009; Revised Manuscript Received January 29, 2010*

**ABSTRACT:** Acid/base and conformational properties of a weak polyelectrolyte chain surrounded by explicit ions (counterions and salt particles) are investigated using Monte Carlo simulations. The influence of the pH, monomer size, presence of explicit ions, salt particles, salt size, and valency on the polyelectrolyte titration process is systematically investigated. It is shown that the presence of explicit ions, the increase in pH and monomer sizes, and the decrease in salt radius are parameters that favor the monomer deprotonation processes hence affecting the global acid/base polyelectrolyte chain properties. The competition between attractive and repulsive, long-range and local electrostatic interactions leads to a heterogeneous distribution of charges and ions along the polyelectrolyte backbones. This subtle electrostatic competition leads to equilibrated chain conformations ranging from extended to globular conformations. A simple screening effect is achieved with monovalent salt resulting in a slight limitation of the formation of extended structures at high pH values. Focusing on trivalent salt, the local complexation of several chain monomers around each trivalent cation leads to the formation of collapsed structures. The decrease in the size of trivalent cations promotes the deprotonation process, in particular, when trivalent salt cations are smaller than the monomer size.

## 1. Introduction

For several years, polyelectrolytes have attracted experimentally and theoretically much attention because of their ionizable groups that are associated with a large range of compounds including charged polymers and macroions such as micelles and biomacromolecules (polysaccharides, proteins, DNA, etc.).<sup>1–6</sup> The range of parameters influencing polyelectrolyte conformation, chemical reactivity, and complexation processes is not completely understood and continues to stimulate intensive research in this field because they control directly many industrial<sup>7–10</sup> and biological processes.<sup>11–14</sup> The particular physicochemical properties of polyelectrolyte chains arise from the long-range nature of the Coulomb interactions. In addition, in the vicinity of chains, small charged mobile counterions interact strongly with the chain backbone, leading to a rich conformational behavior by reducing Coulomb repulsions and introducing ion–ion mediated attractions. For weak polyelectrolytes, the strength of Coulomb interactions (attractive and repulsive) and the presence of counterions in the vicinity of the polyelectrolyte backbone are strongly dependent on the chain degree of ionization and consequently of the pH.

Acid/base properties of isolated monomers and polyelectrolyte chains are not identical. For isolated acid monomers (HA), the chain degree of ionization,  $\alpha$ , and the pH are related to  $pK_0$  by

$$pK_0 = \text{pH} - \log \frac{\alpha}{1 - \alpha} \quad (1)$$

where  $pK_0$  represents the negative logarithm of the dissociation constant of isolated monomers. In the polyelectrolyte chain case, the monomers are connected to each other, and removing a

proton becomes more and more difficult with the increase in the chain degree of ionization. As a result, the dissociation constant  $K$  decreases,<sup>15</sup> and  $\Delta pK$  may be defined as

$$\Delta pK = pK - pK_0 \quad (2)$$

where  $pK$  represents the apparent negative logarithm of the dissociation constant. In fact,  $pK_0$  is the limit of  $pK$  as  $\alpha \rightarrow 0$ .

Weak polyelectrolytes were first experimentally studied by potentiometric titration, and several empirical theories derived from the extended Henderson–Hasselbalch equation<sup>16</sup> were proposed to link together experimental parameters such as  $pK$ , pH, and  $\alpha$ .<sup>17,18</sup> The titration curve shape and apparent proton dissociation constant were found to depend indirectly on many parameters such as the temperature, chain and salt concentrations, or chain charge density. Considering systems with uniform dielectric constants, the titration curves of weak polyacids remain regular with the increase in the ionization degree with pH and  $pK$ . On the other hand, the deprotonation process adopts a different behavior for systems where the dielectric constant of the polyelectrolyte chain is lower than that of the solvent. Such a dielectric discontinuity between the chain and its surroundings results in an increase in the electrostatic interactions leading to the emergence of a plateau in the titration curves near  $\alpha$  equal to 0.5.<sup>19,20</sup> Such a plateau was also described theoretically by Raphael and Joanny<sup>21</sup> as the result of a first-order transition leading to conformational changes between globular and extended state of weak polyelectrolytes in poor solvent. This conformational transition for hydrophobic weak polyelectrolytes was experimentally investigated many years ago by Braud<sup>22</sup> and more recently by Vallat et al.<sup>23</sup> The existence of a plateau in the titration curves was also attributed to electrostatic effects, and a good agreement between theoretical and experimental curves was obtained by including correlations between chain charges in the free energy calculations.<sup>24</sup>

\*To whom correspondence should be addressed. E-mail: serge.stoll@unige.ch.

It should be noted that titration curves of more complicated systems such as humic acids and proteins constitute a valuable tool to identify some functional groups and better understand the complex charging behavior that occurs in heterogeneous natural systems.<sup>25,26</sup>

The effect of the presence of counterions around highly charged polyelectrolytes was widely studied for many years, leading to several theories.<sup>27–34</sup> The classical mean-field approach concerns only repulsive interactions between charged monomers and consequently fails to describe systems containing multivalent counterions or salt particles where ion–ion correlations are strong. In general, the presence of multivalent cations leads to the compaction and precipitation of flexible strongly charged polyelectrolytes followed in some cases by their redissolution at high salt concentration. This collapse was first predicted by González-Mozuelos and Olvera de la Cruz<sup>35</sup> by taking into account short-range attraction between monomers resulting from counterion condensation. For the first time, they showed that correlations ignored by previous models lead to the precipitation of chains; when the charged density of the chains increases, the size of the counterions decreases and/or their valence increases. Compact chains are favored when the effective charge per polyion is nearly zero because such conformations have lower free energy. Later, Solis and Olvera de la Cruz<sup>36,37</sup> proposed a two-state approach: extended or collapsed. The free energy of each state was calculated under specific conditions to determine which state is preferred. For the authors, collapsed conformations are observed when the charges of multivalent particles compensate the ones of the chain. In this state, the polyelectrolyte core is viewed as an amorphous ionic solid. When more salt is added, overcharging is observed, and chains redissolve as expanded-coiled conformations. Using a continuum theory to follow the condensation process of divalent cations, Kundagrami and Muthukumar<sup>38</sup> observed chain contractions to Gaussian size at the isoelectric point. When salt concentration is increased, the chain is overcharged and reswells. For the authors, the electrostatic interactions and dielectric inhomogeneity near the polyelectrolyte backbone are responsible of its charge reversal. Considering rodlike DNA molecules, Nguyen et al.<sup>39</sup> proposed an explanation taking into account condensed and dissolved phases. The phase transition occurs when the chemical potential of DNA in its condensed and dissolved states are equal. Therefore, there exists a range of multivalent salt concentration around the isoelectric point of DNA chains where the energy of short-range attraction dominates the energy of Coulomb repulsion. Below and above this concentration window, chain net charge is negative and positive, leading to dissolved phases.

Monte Carlo (MC) and Molecular Dynamics (MD) simulations are regularly used to fill the gap between theory and experiments. The main tendencies of weak polyelectrolytes are the regular increase in  $\alpha$  with pH and  $\Delta pK$  with  $\alpha$ , thus supporting observed experimental data and theoretical predictions.<sup>40–43</sup> The influence of parameters such as the Debye length, charge spacing, and charge distribution on the chains, salt, and monomer concentration have been systematically investigated. When salt is added, the Debye length decreases. Consequently, the charge interactions on the chains are better reduced, and the ionization process is more successful, thus leading to smaller  $\Delta pK$  values. By decreasing the charge spacing on the chains and the polyelectrolyte concentration, protonation is favored. Moreover, as reported by Limbach and Holm<sup>44</sup> for strongly charged polyelectrolytes, the charge distribution on weak polyelectrolytes is not uniform, and charge accumulation occurs at chain extremities.<sup>45</sup> Concerning highly charged polyelectrolytes, drastic changes of conformations were observed with the variation of the concentration of multivalent particles,<sup>46–50</sup> which is in good agreement with the developed theories.<sup>35–38</sup>

Chain conformations are also widely influenced by their stiffness. Toroidal and hairpin conformations were observed by several groups considering semiflexible chains surrounded by tri- and tetravalent particles.<sup>51–53</sup> Both structures are stable, but toroids are favored as stiffness is increased, suggesting that they may correspond to the global minimum of free energy.

In previous studies, we performed MC simulations to get insight into the conformational behavior of polyacrylic acid chains with different molecular weights.<sup>43</sup> A good correlation between simulated and experimental titration curves was obtained for a large range of  $\alpha$  values when the electrostatic interactions are dominant. In this study, we extend our previous MC simulations with long-range Coulomb potential in the grand canonical ensemble to gain insight into the influence of the explicit description of ions (counterions and salt particles), monomer radius, and presence of divalent and trivalent explicit cations on the titration curves of weak polyelectrolyte chains. Local and long-range effects due to the presence of explicit ions mediated by pH variations are expected to influence significantly in a nonlinear way the titration curves.

The article is organized as follows: the model and MC procedure are presented first. Chain conformations in a salt-free environment during the titration process are briefly presented. Salt is then added, and the differences between chain conformations with mono-, di-, and trivalent salts are discussed by considering an identical salt concentration. In addition, the effect of trivalent cation sizes is analyzed in detail. In the last section, the influence of an identical ionic strength (and not salt concentration) is examined.

## 2. Model and Monte Carlo Simulations

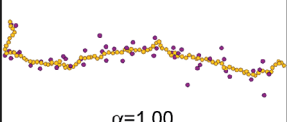
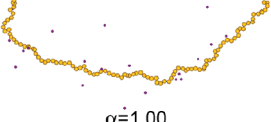
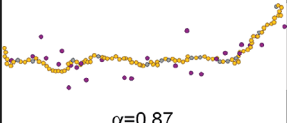
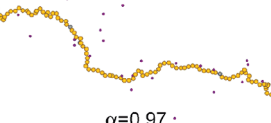
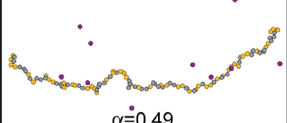
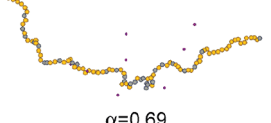
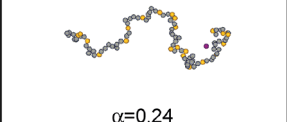
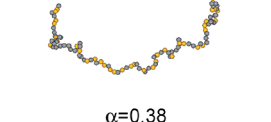
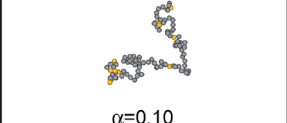
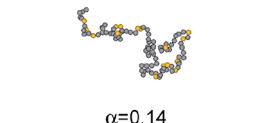
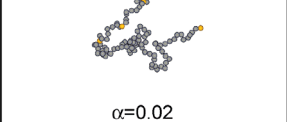
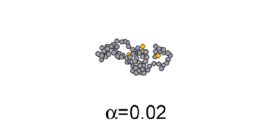
A coarse-grained model is used to describe the system. Polyelectrolyte chains are represented as a succession of  $N$  off-lattice 3D freely jointed hard spheres. Monomers can be negatively charged ( $-1$ ) or neutral, depending on the pH. The ions surrounding the chains (counterions and salt) are impenetrable charged spheres. The surrounding ions carry always a charge ( $+1$  for the counterions,  $+1$ ,  $+2$ , or  $+3$  for the salt cations, and  $-1$  for the salt anions). The solvent, here water, is treated implicitly as a dielectric medium, and the simulations are performed at 298 K in a cubic box. The monomer radius is adjusted to 2 (model A) and 3.57 Å (model B). Model B was chosen so as to be out of the Manning counterion condensation domain in the full range of the chain degree of ionization  $\alpha$ , whereas counterion condensation is expected to occur when  $\alpha > 0.56$  in model A.<sup>27</sup> The counterion and salt anion radii are fixed to 2 Å for the whole study, whereas the salt cation radii are fixed to 2 and 2.5 for mono- and divalent salts, respectively. The trivalent salt cation radius may vary within the range of 1.5–4 Å.

All pairs of charged monomers and ions interact with each other via a long-range Coulomb electrostatic potential and a hard-sphere repulsion according to

$$U_{ij}(r_{ij}) = \begin{cases} \infty, & r_{ij} < R_i + R_j \\ \frac{z_i z_j e^2}{4\pi\epsilon_0\epsilon_r r_{ij}}, & r_{ij} \geq R_i + R_j \end{cases} \quad (3)$$

where  $e$  is the elementary charge ( $1.6 \times 10^{-19}$  C),  $\epsilon_0$  is the permittivity of the vacuum ( $8.85 \times 10^{-12}$  CV<sup>-1</sup> m<sup>-1</sup>),  $\epsilon_r$  is the relative dielectric constant of solvent (78.54),  $z_{i,j}$  is the charge carried by monomers or ions,  $r_{ij}$  is the distance between them, and  $R_{i,j}$  is their radii. This electrostatic potential is repulsive (positive) for species with charges of same sign and attractive (negative) if the species carry opposite charges. The total energy is the sum of the whole pairwise potentials between monomers, monomers and ions, and between ions.

**Table 1. MC Equilibrated Conformations of Polyelectrolyte Chains Composed of 100 Monomers of Radius 2 (Model A) and 3.57 Å (Model B)<sup>a</sup>**

		Monomer radius [Å]	
		2 (model A)	3.57 (model B)
pH - pK <sub>0</sub>	6	 $\alpha=1.00$	 $\alpha=1.00$
	4.5	 $\alpha=0.87$	 $\alpha=0.97$
	3	 $\alpha=0.49$	 $\alpha=0.69$
	1.5	 $\alpha=0.24$	 $\alpha=0.38$
	0	 $\alpha=0.10$	 $\alpha=0.14$
	-1.5	 $\alpha=0.02$	 $\alpha=0.02$

<sup>a</sup> Each monomer can carry one negative charge (yellow sphere) or can be neutral (grey sphere) depending on the pH. Simulations with monovalent counterions of radius 2 Å are considered here (purple sphere). The degree of ionization,  $\alpha$ , is calculated as a function of the pH-pK<sub>0</sub> parameter. Folded conformations that are achieved at low pH-pK<sub>0</sub> continuously expand with pH-pK<sub>0</sub> increase to minimize the electrostatic energy of the system. Monovalent counterions are more attracted at high pH-pK<sub>0</sub> values and by the chain having a monomer radius equal to 2 Å.

MC simulations are performed according to the Metropolis algorithm in the grand canonical ensemble.<sup>54</sup> The polyelectrolyte position is modified by specific movements (kink-jump, end-bond, reptation, and partially clothed pivot<sup>55–57</sup>). All counterions and salt particles are moved through the box by translation movements. The acceptance of each protonation/deprotonation step is related to the MC metropolis selection criterion as follows<sup>40</sup>

$$\Delta E = \Delta E_{\text{tot}} \pm k_B T \ln 10 (\text{pH} - \text{p}K_0) \quad (4)$$

where  $k_B$  is the Boltzmann constant ( $1.3807 \times 10^{-23} \text{ J K}^{-1}$ ) and  $T$  is the temperature (298 K). The minus sign is used when the monomer is deprotonated, and the plus sign is used when the monomer is protonated. In the simulations, pH-pK<sub>0</sub> is an input parameter, and the simulation box is coupled to a proton bath to establish a constant pH. Because simulations are performed in a grand canonical ensemble, the box volume, the temperature, and the chemical potential remain constant. The particle number may vary during the simulation process. After each 10 000 MC step cycles to achieve the conformational chain relaxation, each N/8

monomer charge is switched on if the monomer is neutral or inversely if it is charged. Because the box remains electrostatically neutral, if a charge appears on the chain, an oppositely charged particle (counterion) is inserted randomly into the box or removed if a charge disappears. The explicit added counterion is resulting from the addition of an alkali such as NaOH. After the equilibration period, which is  $\sim 5 \times 10^5$  MC steps for a given pH-pK<sub>0</sub>, observables such as the chain degree of ionization,  $\alpha$ , or the distance between monomers and ions are recorded to calculate average values for the whole  $2 \times 10^6$  MC steps.

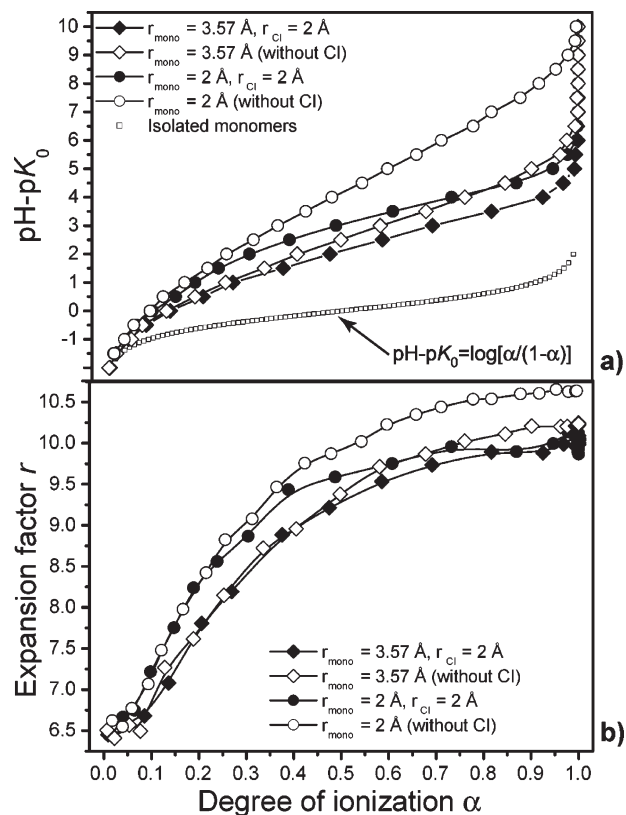
### 3. Results and Discussion

**3.1. Salt-Free Case.** We investigate first the case of an isolated weak polyelectrolyte surrounded by its explicit counterions. Chains composed of 100 monomers of radius 2 (model A) and 3.57 Å (model B) are considered. Equilibrated conformations are presented in Table 1 for various monomer radii and pH-pK<sub>0</sub> values. In the inset of each cell,  $\alpha$  represents the average value of the chain degree of ionization. Globally, the increase in pH-pK<sub>0</sub> makes the deprotonation process more effective. The degree of ionization increases in both cases to  $\alpha = 1$ , and extended structures are achieved to minimize the long-range electrostatic energy of the polyelectrolyte chain. During the increase in the pH-pK<sub>0</sub> value, the monomer-monomer repulsive interactions are in competition with attractive monomer-counterion interactions. The monovalent counterions that appear during the chain deprotonation are attracted by the chain, in particular, with model A, but not strongly enough to counterbalance the repulsive monomer-monomer interactions. As a result, the chains expand and important conformational changes (such as polyelectrolyte collapse) at a high degree of ionization do not occur. At low pH-pK<sub>0</sub>, the chains remain almost neutral, and folded structures are observed. For a given pH-pK<sub>0</sub> value, the chain deprotonation process is less efficient for model A than for model B. Also when the monomer size is increased at high dissociation degree, the counterions are diluted away from the polyelectrolyte chain, thus increasing the “net charge” and subsequently the dimension of the polyelectrolyte.

**Titration Curves.** Titration curves for the two chain models A and B are presented in Figure 1a. For comparison, titration curves for chains without counterions and for isolated monomers are also given. Simulations for chains without counterions are carried out in a non-neutral cubic box. Curves fit only with the isolated monomer curve when the chains are close to neutrality. By increasing the degree of ionization,  $\Delta pK$  becomes rapidly more and more important. By focusing on the curves without counterions (open symbols), we observe an important difference between them. Indeed, repulsive electrostatic interactions are stronger between monomers in model A than monomers in model B. Consequently, the curves with 2 Å monomers are systematically above the ones with 3.57 Å monomers. Such a behavior is also observed for the simulations with counterions (filled symbols). In this case, the difference between the two models with counterions remains limited because the explicit counterions introduce attractive electrostatic interactions that counterbalance the repulsive chain energy, thus leading to a local charge screening effect of the intramolecular chain interactions. Consequently, the deprotonation is easier for a chain surrounded by its counterions. In this case, the deviation from the ideal case is less pronounced than without counterions.

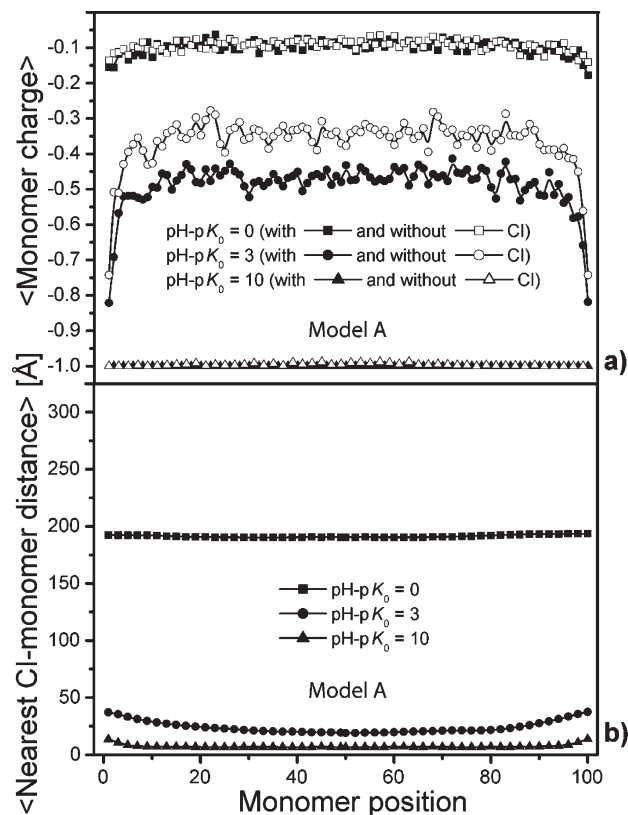
**Conformational Properties.** To get insight into the conformational properties of the polyelectrolyte chains,





**Figure 1.** (a) Monte Carlo titration curves and (b) expansion factor calculated as a function of  $\alpha$  for polyelectrolyte chains composed of 100 monomers of radius 2 (model A) and 3.57 Å (model B). Cases without explicit counterions and with monovalent counterions of radius 2 Å are considered. Parameters that favor the deprotonation process are the increase in  $\text{pH} - \text{p}K_0$ , the presence of explicit counterions, and the increase in the monomer radius. In part b, the presence of explicit counterions limits the chain expansion, resulting in the formation of a plateau with the increase in  $\alpha$ .

parameters such as the expansion factor  $r = \langle R_{\text{ee}}^2 \rangle / \langle R_{\text{g}}^2 \rangle$ , the mean monomer charge, and the mean nearest counterion–monomer distance are calculated. Figure 1b represents the expansion factor,  $r$ , of the polyelectrolyte chains for models A and B. When  $\alpha$  is close to 0, small expansion factors are found. For models A and B,  $r = [6.4, 6.5]$  for chains with and without counterions. These expansion factors are close to 6.3 and are in good agreement with the self-avoiding walk (SAW) model considering excluded volume chains.<sup>58</sup> By increasing further the degree of ionization, the expansion factors increase rapidly and then reach asymptotic values at  $\sim 10$  for simulations with counterions (for both monomer radii) and 10.2 and 10.6 for simulations without counterions for models B and A, respectively. The absence of counterions leads to a regular decrease in the slope of the curves (open symbols) by increasing the degree of ionization. Moreover, the difference between the asymptotic values of models A and B, achieved when  $\alpha$  is close to 1, confirms the monomer size effects. The influence of the counterions is more visible on model A than on model B (filled symbols). Furthermore, the decrease in the curve slope is regular for model B, whereas an important change is observed at an ionization degree of 0.39 for model A. This phenomenon results from counterion condensation, which is higher for 2 Å monomer radii. In our case, but for infinitely rigid rods, Manning theory<sup>27</sup> predicts a counterion condensation only for 2 Å monomer radii starting at an ionization degree of 0.56 up to 1. This range of  $\alpha$  corresponds to the domain of the 2 Å monomer radius

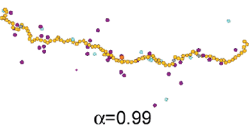
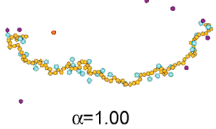
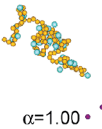
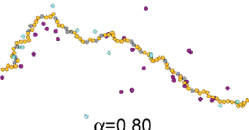
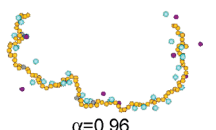
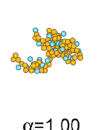
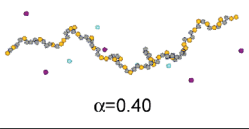
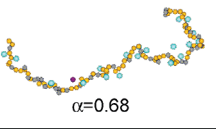
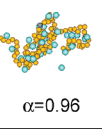
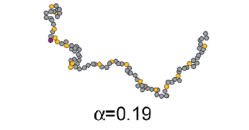
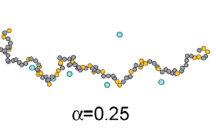
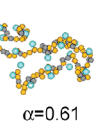
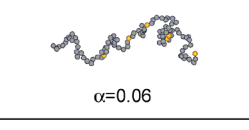
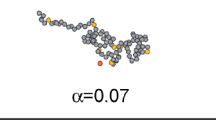
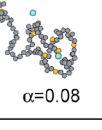
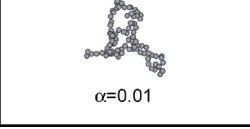
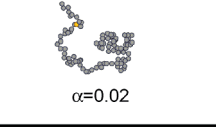
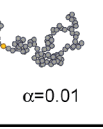


**Figure 2.** (a) Mean monomer charge and (b) nearest counterion–monomer distance calculated as a function of the monomer position for polyelectrolyte chains composed of 100 monomers of radius 2 Å. In part a,  $\text{pH} - \text{p}K_0 = 0, 3$ , and 10, and simulations with and without monovalent counterions are considered, whereas the case with only monovalent counterions is presented in part b. The mean monomer charge varies from 0 (protonated) to  $-1$  (fully deprotonated). The charge and counterions distribution are not uniform along the chains. The mean monomer charge becomes more important at the chain extremities, showing a better deprotonation. The presence of explicit counterions is also promoting deprotonation. Even if more charges appear at the chain extremities, the counterions are more attracted by the central part of the chains.

curve where the slope changes toward the formation of a plateau (ionization degree above 0.39).

To capture the main features of charge distribution at the polyelectrolyte chains and ion distribution around them, the mean monomer charge and mean nearest counterion–monomer distance are calculated. Figure 2a represents the mean monomer charge of model A. Curves with and without counterions for  $\text{pH} - \text{p}K_0$  values of 0, 3, and 10 are given. The charge distribution is found to be not uniform along the chains, which is in good agreement with other studies.<sup>45</sup> At low  $\text{pH} - \text{p}K_0$ , the chains remain almost neutral. By increasing  $\text{pH} - \text{p}K_0$ , the mean monomer charge becomes significantly more important at the chain extremities, showing a better deprotonation. For instance, when  $\text{pH} - \text{p}K_0 = 3$ , the mean value at the center of the chain is equal to  $-0.47$  for simulations with counterions, whereas the mean charge values decrease to  $-0.82$  at the chain extremities. This heterogeneous charge distribution disappears at high  $\text{pH} - \text{p}K_0$  values when chains are totally deprotonated (mean monomer charge equal to  $-1$  for the whole monomers). Considering larger monomers, the same global shape is obtained with minor differences (figure not shown here). First, the values at the center of the chain are lower, meaning that deprotonation is favored in this case. Second, the difference between the mean values at the chain center and

**Table 2.** Equilibrated Conformations of Polyelectrolyte Chains Composed of 100 Monomers of Radius 2 Å (Model A)<sup>a</sup>

		Model A, $C_i = 1 \times 10^{-4}$ [M]		
		Monovalent salt	Divalent salt	Trivalent salt
pH - pK <sub>0</sub>	5.5	 $\alpha = 0.99$	 $\alpha = 1.00$	 $\alpha = 1.00$
	4	 $\alpha = 0.80$	 $\alpha = 0.96$	 $\alpha = 1.00$
	2.5	 $\alpha = 0.40$	 $\alpha = 0.68$	 $\alpha = 0.96$
	1	 $\alpha = 0.19$	 $\alpha = 0.25$	 $\alpha = 0.61$
	-0.5	 $\alpha = 0.06$	 $\alpha = 0.07$	 $\alpha = 0.08$
	-2	 $\alpha = 0.01$	 $\alpha = 0.02$	 $\alpha = 0.01$

<sup>a</sup> Yellow monomers are negatively charged ( $-1$ ) and grey ones are neutral. Chain monovalent counterions of radius 2 Å are purple. The cases with mono-, di-, or trivalent salts of radius 2, 2.5, and 2.5 Å (cyan spheres) are considered here. Salt concentration is fixed at  $1 \times 10^{-4}$  M. The chain conformations vary from folded to extended with the increase in pH-pK<sub>0</sub> with mono- and divalent salts. At the opposite, folded conformations are achieved with trivalent salt even at high pH-pK<sub>0</sub>, showing a strong complexation between the salt cations and chain monomers.

at the extremities is lower when deprotonation is favored. Consequently, the end effects are much more important for small monomers, where repulsive electrostatic interactions between charged sites are strong.

The explicit presence of counterions also plays a significant role in the protonation/deprotonation process. In Figure 2a, the mean plateau values are identical for simulations with and without counterions when the polyelectrolyte chains are almost neutral or fully deprotonated, which is not the case for intermediate pH-pK<sub>0</sub> values. Indeed, at pH-pK<sub>0</sub> = 3, the mean plateau values are equal to -0.47 with counterions and -0.34 without counterions. This result shows that deprotonation is promoted by the explicit presence of counterions and larger monomers.

The counterion distribution around the chains is now investigated. Figure 2b represents the mean nearest distance from each monomer for model A at pH-pK<sub>0</sub> values equal to 0, 3, and 10. When pH-pK<sub>0</sub> = 0, because of the quasi-neutrality of the chains, the counterions are not attracted and occupy the whole space. In the central part of the chain, the mean nearest counterion-monomer distance is equal to

19.10 Å at pH-pK<sub>0</sub> = 3. When pH-pK<sub>0</sub> = 10, this distance falls to 6.61 Å. Similar to the monomer charge distribution, the counterions are not uniformly distributed around the chain. They are attracted by the central part of the chains, in good agreement with the molecular dynamics simulations of Limbach and Holm.<sup>44</sup> It is interesting to note that on one hand the monomers situated at the chain extremities carry more charges whereas on the other hand counterions are more attracted by the central part of the chains. Indeed, the attractive electrostatic interactions between the counterions and polyelectrolytes are more important with the central part of the chains because they involve most of the monomers.

**3.2. Constant Salt Concentration Case.** The case of an isolated weak polyelectrolyte surrounded by its explicit counterions (monovalent) and salt particles is now investigated. Only model A is considered in the following. Salt concentration is fixed to  $1 \times 10^{-4}$  M for the whole simulation, whereas the ionic strength varies from  $1 \times 10^{-4}$  for monovalent to  $3.46 \times 10^{-2}$  M for trivalent salt. We focus here on the influence of the mono-, di-, and trivalent salts (radii = 2, 2.5, and 2.5 Å) and pH on the protonation/deprotonation

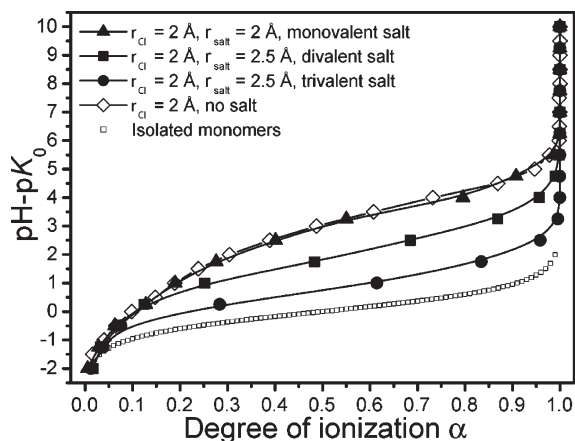


**Figure 3.** Titration curves for polyelectrolyte chains composed of 100 monomers of radius 2 Å. Cases with explicit monovalent counterions (radius = 2 Å) and explicit mono-, di-, or trivalent salts (radii = 2, 2.5, and 2.5 Å) are considered. Salt concentration is fixed at  $1 \times 10^{-4} \text{ M}$ . Monovalent salt has little effect in comparison to the situation without salt. A shift is observed toward the ideal curve for simulations with multivalent salt leading to higher  $\alpha$  values for a given  $\text{pH}-\text{p}K_0$ .

process. Equilibrated conformations are represented in Table 2 for the mono-, di-, and trivalent salts and different  $\text{pH}-\text{p}K_0$  values. Inside the snapshots,  $\alpha$  represents the mean chain degree of ionization. Globally, the deprotonation process is improved by the increase in  $\text{pH}-\text{p}K_0$  values for each ionic strength. For the mono- and divalent salts, the chain conformations are quantitatively close to the ones without salt. Indeed, chain conformations change progressively from SAW at low  $\text{pH}-\text{p}K_0$  to stretched structures at high  $\text{pH}-\text{p}K_0$  values. Folded structures are achieved with the trivalent salt even at high  $\text{pH}-\text{p}K_0$  values, in good agreement with other MC and MD simulation studies dealing with strong polyelectrolytes.<sup>47–49</sup>

Monomer–trivalent salt cation attractive interactions are strong enough to counterbalance the monomer–monomer repulsive interactions. Furthermore, as shown in Table 2, the trivalent salt cations take the place of the monovalent counterions, which were surrounding the chains. Because of the strong monovalent counterion–trivalent salt cation repulsive interactions and competition between the different ions species, the monovalent counterions rise up into the bulk. By comparing the different salts and chain degree of ionization, we observe that for a given  $\text{pH}-\text{p}K_0$  value and salt concentration, the increase in the ionic strength (from mono- to trivalent salt) makes the deprotonation process leading to higher ionization degrees easier.

**Titration Curves.** Titration curves for model A are presented in Figure 3. For comparison, titration curves without salt (only monovalent counterions) are also given. Titration curves considering di- and trivalent salts are found to be situated between the one without salt and the ideal curve. Monovalent salt has little influence at such a salt concentration. By increasing salt valency, a significant shift is observed, and the curves for di- and trivalent salts are found below the one with monovalent salt. The presence of di- and trivalent salt cations in the vicinity of the chains clearly promotes the chain degree of ionization. Furthermore, the difference between calculated and ideal curves is reduced with increasing salt valency.

**Conformational Properties.** The influence of salt valency on the conformational properties of the polyelectrolyte chains is now investigated. The term “ion” describes in this section the monovalent counterions and the salt cations.

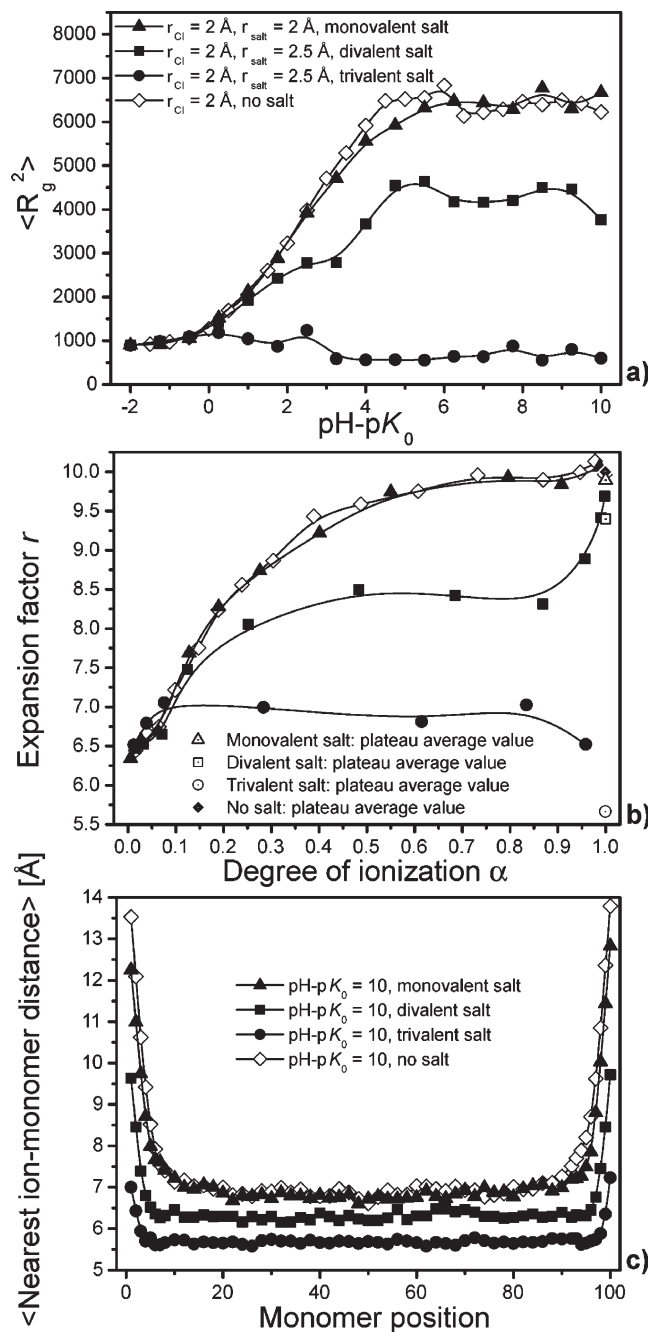


**Figure 4.** (a) Polyelectrolyte mean-square radius of gyration  $\langle R_g^2 \rangle$ , (b) expansion factor, and (c) mean nearest ion–monomer distance for chains of 100 monomers (radius = 2 Å). The term “ion” describes the monovalent counterions and the salt cations. Trivalent salt cations have strong attractive interactions within the chains and are adsorbed by several monomers leading to the decrease in  $\langle R_g^2 \rangle$  and limiting the expansion factor. The distance between trivalent cations and chain is thus smaller than with mono- and divalent salts.

Results for simulations with no salt (only monovalent counterions) are also given for comparison. The mean-square radius of gyration  $\langle R_g^2 \rangle$  as a function of  $\text{pH}-\text{p}K_0$  is presented in Figure 4a for model A.  $\langle R_g^2 \rangle$  increases continuously with  $\text{pH}-\text{p}K_0$  and then reaches a plateau value for simulations without and with mono- and divalent salts. Such variations indicate an increase in the chain dimensions.

Considering trivalent salt, an opposite trend is observed. Indeed,  $\langle R_g^2 \rangle$  starts first to decrease then reaches a plateau value indicating that collapsed conformations are formed with an increase of  $\text{pH}-\text{p}K_0$ . It should be noted that

fluctuations are observed around the plateau values. This is due to the fact that molecules are not frozen, hence resulting in continuous thermal fluctuations of chain dimensions. During the titration process, attractive and repulsive electrostatic interactions are continuously in competition. Once attractive interactions between the chain backbone and the salt cations are strong enough (for a given ionization degree), then salt cation condensation is obtained. This can be put in evidence by the formation of an asymptotic regime (plateau) on the curves.

For simulations without and with monovalent salt, the counterions and salt particles have an electrostatic screening effect only leading to extended chain structures. At the opposite, the electrostatic interactions between monomers and trivalent salt cations are strong enough to form collapsed structures, even at low  $\text{pH}-\text{p}K_0$  values. Indeed, each trivalent salt cation, in this case, is adsorbed by several chain monomers, hence explaining the decrease in the curve with trivalent salt. For simulations with divalent salt, an intermediate behavior is obtained because  $\langle R_g^2 \rangle$  values are found between the ones for mono- and trivalent salts. Compared with monovalent salt, divalency promotes salt adsorption by monomers but remains quite limited. Only a few salt particles form strong complexes with several monomers, leading to very local folded structures. (See Table 2 at  $\text{pH}-\text{p}K_0 = 4$ ). The competition between cation–monomer complexation and chain thermal movements gives higher fluctuations of the plateau values in comparison with mono- and trivalent salts. Divalent salt is then responsible for a subtle competition between intramolecular electrostatic screening and complexation processes.

Complementary information on the conformational changes versus the salt valency is obtained by representing the expansion factor as a function of the degree of ionization (Figure 4b). For clarity, the  $\alpha$  and expansion factors corresponding to the  $\text{pH}-\text{p}K_0$  values at the plateau in Figure 4a are summed for each curve, and the mean values are given using the same symbol but with opposite color (last points of the curves at  $\alpha \approx 1$ ). By increasing  $\alpha$  from 0 to 1, an important and continuous chain expansion is observed for mono- and divalent salts with the maximum value reached at about  $\alpha = 1$ .

The conformational changes are different for simulation with the trivalent salt because the chain expansion is rapidly limited by the presence of salt cations. Indeed, the expansion factor quickly increases until 7 and fluctuates slightly around this value until  $\alpha = 0.85$  and finally decreases strongly to reach an expansion factor equal to 5.7 smaller than the one of the SAW chain. This behavior confirms that trivalent salt interacts strongly with monomers, leading to collapsed structures that become very compact when  $\alpha$  is close to one. During the titration process, no chain reexpansion is observed with the increase in  $\alpha$ . As observed by others groups by MC and MD simulations of strongly charged polyelectrolytes with multivalent salt,<sup>47,49</sup> a reexpansion occurs when the whole salt cation charges overcompensate the charges of the chain. The salt concentration used in this section is low and does not allow us to reach this situation.

Monovalent salt cations, which cannot be physically distinguished from monovalent counterions, lead to the superimposition of the curves with the situation without salt. In this case, the expansion factor regularly increases to reach a maximum value equal to 10. The intermediate case with divalent salt allows us to obtain initially a stabilization of the chain expansion (plateau value at  $\sim 8.4$ ). With the increase in  $\alpha$  to values  $> 0.9$ , repulsive electrostatic interactions between the monomers become strong enough to destabilize the

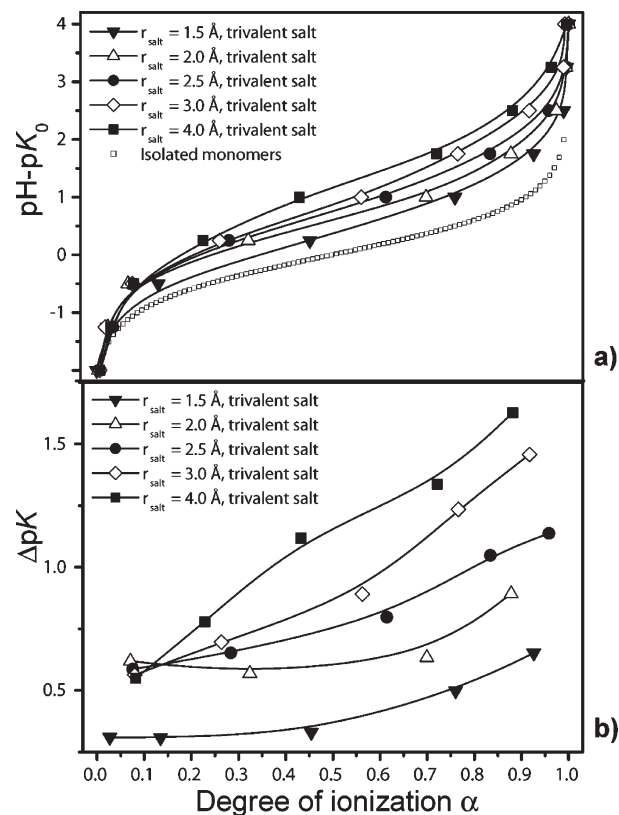


**Figure 5.** (a) Titration curves and (b)  $\Delta\text{p}K$  for chains composed of 100 monomers (radius = 2 Å) surrounded by explicit monovalent counterions (radius = 2 Å) and trivalent salt cations of concentration  $1 \times 10^{-4}$  M. The radius of salt cations is adjusted from 1.5 to 4 Å. The deprotonation process is promoted by decreasing the size of trivalent ions.  $\Delta\text{p}K$  increases with  $\alpha$ , and the corresponding slopes are increasing concomitantly with the trivalent ion radius showing a lower efficiency of the deprotonation process.

structures, and the expansion factor increases rapidly to reach a value in the same range as simulations with monovalent salt. As a result, for full deprotonated chains, extended structures are also observed. By comparing the nearest ion–monomer distance when  $\text{pH}-\text{p}K_0 = 10$  and  $\alpha = 1$  in Figure 4c, it is found that collapsed structures correspond to the smaller mean distance. The repulsive energy of trivalent salt particles between themselves is then not strong enough to separate them from the polyelectrolyte chains, even if distances between adsorbed trivalent salt cations are small. Salt valency has no influence on the heterogeneous distribution of the counterions and salt cations around the polyelectrolytes. Indeed, they are always more attracted to the central part of the chains, and the end effects remain present with mono-, di-, and trivalent salts.

**Effect of Trivalent Salt Particle Sizes.** The effect of the size of trivalent ions is now investigated by considering salt particles with cation radius ranging from 1.5 to 4 Å. Salt concentration is fixed to  $1 \times 10^{-4}$  M. The titration curves and  $\Delta\text{p}K$  variations as a function of the degree of ionization are represented in Figure 5. Ion size plays a significant role in the global shape of titration curves. For instance, when  $\text{pH}-\text{p}K_0 = 1$ , the difference in  $\alpha$  between salt cation radii of 1.5 and 4 Å reaches 0.33. In the whole  $\alpha$  range, the deprotonation process is promoted by decreasing the size of trivalent ions. The attractive electrostatic interactions with the chain are stronger, leading to a better screening of the intramolecular chain interactions. This result is in good agreement with the two state model of Solis and Olvera de la Cruz<sup>36</sup> for highly



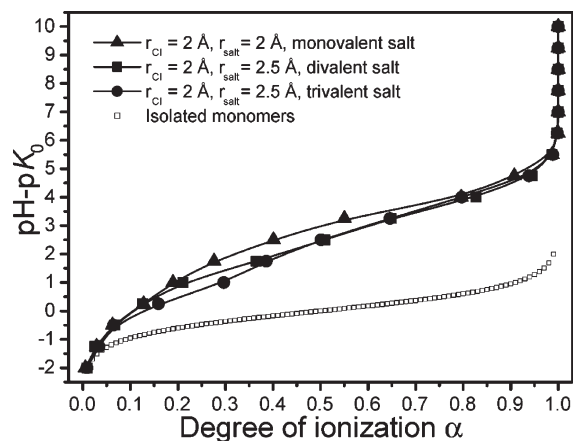


**Figure 6.** Titration curves for polyelectrolyte chains composed of 100 monomers of radius 2 Å. Cases with explicit monovalent counterions (radius = 2 Å) and mono-, di-, or trivalent salts (radii = 2, 2.5, and 2.5 Å) are considered. The ionic strength is fixed at  $1 \times 10^{-4}$  M. Curves are not distinguishable for neutral and fully charged chains. For an intermediate  $\alpha$  range, salt multivalency promotes the deprotonation process, leading to a significant shift in titration curves.

charged polyelectrolytes where the effective ionic glass cohesive energy is inversely proportional to the ion size.  $\Delta pK$  variations (Figure 5b) put in evidence the differences between trivalent cations, in particular, when they are smaller than the polyelectrolyte monomers. For cation radii of 2.5, 3, and 4 Å,  $\Delta pK$  values are about 0.6 when  $\alpha = 0.1$  and increase regularly with the degree of ionization. The corresponding slopes are increasing concomitantly with the trivalent ion radius showing a lower efficiency of the deprotonation process due to the importance of the excluded volume. When  $r_{\text{salt}} = 2$  Å, the trivalent cations limit the increase in the chain electrostatic energy with  $\Delta pK$  values quasi-constant in the range of  $\alpha = [0, 0.45]$ . For higher degrees of ionization, the increase in polyelectrolyte monomer–monomer repulsive interactions is no more compensated by the presence of small cations. When  $r_{\text{salt}} = 1.5$  Å, that is, less than the polyelectrolyte monomer radius,  $\Delta pK$  is significantly less important, in particular, at low degree of ionization. Because of a possible reduced distance between the cations and the charged monomers, the strong electrostatic interactions allow us to obtain  $\Delta pK$  values of  $\sim 0.3$  within the range  $\alpha = [0, 0.45]$  and then increasing regularly to reach 0.65 for  $\alpha = 0.92$ . Salt cations of radius 1.5 Å are then of particular interest because they modify significantly the acid/base properties of the polyelectrolyte chains, even at low degree of ionization.

**3.3. Constant Ionic Strength Case.** An isolated weak polyelectrolyte surrounded by its explicit counterions (monovalent) and salt particles (mono-, di-, and trivalent of radii = 2, 2.5, and 2.5 Å) is investigated in this section. Chains are composed of monomers of radius 2 Å (model A), and the salt ionic strength is fixed to  $1 \times 10^{-4}$  M for the whole simulation runs. We focused here on the influence of the ion valency at a given ionic strength on the protonation/deprotonation process, and comparisons are made with simulations of Section 3.2, where the ionic strength is variable for a given salt concentration.

**Titration Curves.** Titration curves are presented in Figure 6 for model A. A significant shift is observed for simulations with di- and trivalent salts in the range of  $\text{pH}-\text{p}K_0$  (−0.5 to 4.0), where multivalency improves the chain deprotonation process. As expected, the monovalent and trivalent salt curves represent the upper and lower limits, and the divalent salt is situated in

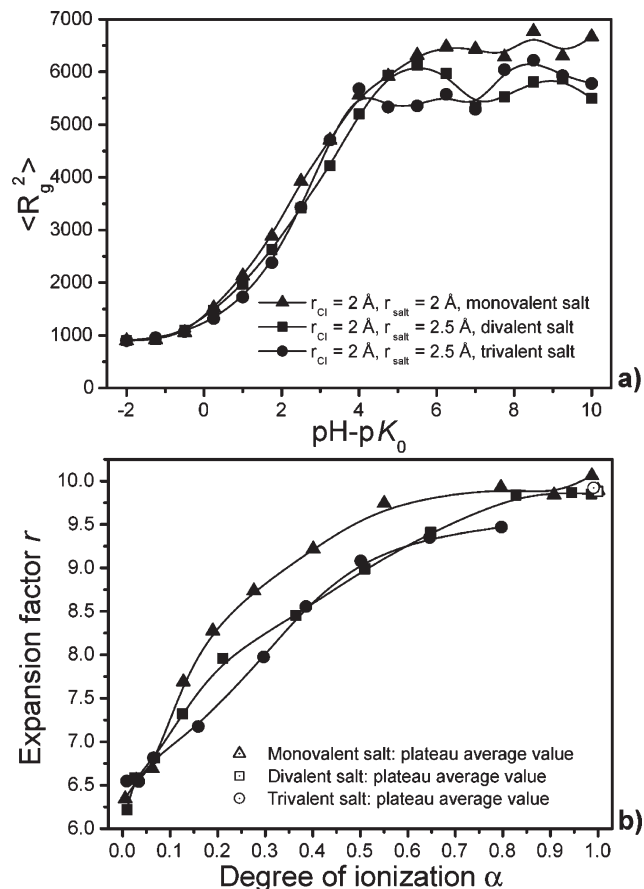


**Figure 7.** (a) Mean-square radius of gyration  $\langle R_g^2 \rangle$  as a function of  $\text{pH}-\text{p}K_0$  and (b) expansion factor as a function of  $\alpha$  for chains of 100 monomers (radius = 2 Å) surrounded by explicit monovalent counterions (radius = 2 Å) and mono-, di-, or trivalent salts (radii = 2, 2.5, and 2.5 Å).  $\langle R_g^2 \rangle$  and the expansion factor increase regularly until plateau values for the different salts. Interactions of di- and trivalent salt cations with the chains are stronger than those with monovalent salt, leading to lower expansion factors and  $\langle R_g^2 \rangle$  plateau values. Extended conformations are achieved at high  $\text{pH}-\text{p}K_0$  values, even for simulations with trivalent salt.

between. At low  $\text{pH}-\text{p}K_0$  values (from −2 to −0.5), multivalency does not have any influence, and the curves are not distinguishable. By increasing  $\text{pH}-\text{p}K_0$ , the affinity of multivalent salt cations becomes stronger with the chains, and a shift of the curves with tri- and then divalent salts is observed. For divalent salt, the influence of cations in the deprotonation process is the same as that of the monovalent ones in the range of  $\text{pH}-\text{p}K_0$  (−2.0 to 0.25) and changes when  $\text{pH}-\text{p}K_0$  reaches 2.5 to be identical to trivalent salt. At high  $\text{pH}-\text{p}K_0$  values, a superimposition of the curves for mono-, di-, and trivalent salts appears again. By comparing with Section 3.2, the variation of the salt ionic strength considered in Figure 3 has much more influence on titration curves than the variation of the salt concentration in Figure 6. It has to be pointed out that the salt concentrations used here remains low and that one multivalent salt cation has more influence on the deprotonation process than several monovalent ones.

**Conformational Properties.** Conformational properties of the polyelectrolyte chains are investigated here by calculating the mean-square radius of gyration ( $\langle R_g^2 \rangle$ ) and the expansion factor (Figure 7a,b). By investigating the mean-square radius of gyration, a common characteristic is the increase in  $\langle R_g^2 \rangle$  with  $\text{pH}-\text{p}K_0$  until a plateau value at  $\sim 6500$  Å<sup>2</sup> for mono- and  $5700$  Å<sup>2</sup> for di- and trivalent salts. In comparison with Figure 6a, the difference at a given ionic strength



between the different salts is not so important here. Indeed, the chains remain extended at high  $\text{pH}-\text{p}K_0$  values, even for trivalent salt, and no chain collapse is observed. In Figure 7a, di- and trivalent salts lead to lower plateau values, whereas strong fluctuations around the mean values are observed. Owing to the constant ionic strength, a small number of di- and trivalent salt cations are present in comparison with the chain monomer number, thus explaining the strong fluctuations of the plateau values. Moreover, no local complexation with monomers is observed for the different salts. The main effect corresponds here to a simple screening of monomer interactions, which is less successful for monovalent salt.

Such a behavior is supported by the calculation of the expansion factors of the polyelectrolyte chains (Figure 7b). Mean values of the expansion factors and  $\alpha$  corresponding to the  $\text{pH}-\text{p}K_0$  values of the plateau of  $\langle R_g^2 \rangle$  obtained from Figure 7a are calculated. The shape of the different curves is quite similar, and a regular increase in the expansion factors with  $\alpha$  is observed. The mean values of the expansion factors are  $\sim 9.9$  for mono-, di-, and trivalent salts, confirming that extended conformations are reached at high degree of ionization. The effects of di- and trivalent salt cations on the polyelectrolyte are more important, leading to better screening of the intramolecular interactions. As a result, the expansion factors are lower for almost the whole  $\alpha$  range but remain identical when chains are neutral or fully charged. Because equilibrated conformations are quite identical for mono-, di-, and trivalent salts, no significant change of the curve slopes is observed in comparison with Figure 4b.

#### 4. Conclusions

A Coulomb electrostatic potential was used to investigate by MC simulations the acid/base properties of weak polyelectrolyte chains surrounded by explicit counterions and salt particles. Structural properties such as the monomer size were investigated, and we focused on the influence of explicit counterions and salt particles on the protonation/deprotonation process and associated conformational changes. Our simulations point out the importance of several competing effects. On one hand, the electrostatic repulsions along the polyelectrolyte chain increase with the  $\text{pH}$ , which favors the chain deprotonation and chain expansion. On the other hand, explicit counterions and salt particles accumulate close to the polyelectrolyte backbone and limit the intramolecular interactions. As a result, the chain expansion is not only controlled with the increase in  $\text{pH}$  but also with counterions and coions interactions. The analysis of the titration curves, radius of gyration, and expansion factor clearly demonstrate the role of explicit particles in solution. The deprotonation process is facilitated by the presence of oppositely charged ions in solution. Furthermore, the attractive electrostatic interactions of salt particles with the polyelectrolyte chains are more important with multivalent and smaller salt cations, hence amplifying chain deprotonation. Different situations are achieved considering mono-, di-, or trivalent salts. Monovalent salt particles induce a screening effect of the intramolecular interactions, which slightly limits the formation of extended structures at high  $\text{pH}$  values.

Considering trivalent salt, collapsed structures are observed because of the formation of strong complexes between polyelectrolyte monomers and trivalent cations. Salt cation size plays a significant role in the acid/base properties of the polyelectrolyte chains, in particular, when the trivalent cation radius is smaller than the monomer radius. Divalent salt constitutes an intermediate case where a subtle competition between intramolecular electrostatic screening and local effects

is observed. The simulations reported here constitute a preliminary step to understand the exact role of explicit counterions and salt particles in the formation of weak polyelectrolyte assembled systems. Our model is expected to capture the conformational changes of one polymer chain composed of different monomer sizes surrounded by explicit counterions in salt-free and salty environments including  $\text{pH}$  modification effects.

**Acknowledgment.** We express our thanks to Marianne Seijo, Daniel Palomino, and G. S. Manning for their encouragements and stimulating discussions. We also gratefully acknowledge the financial support received from the following source: le Département de l'Instruction Publique de l'Etat de Genève.

#### References and Notes

- (1) Oosawa, F. *Polyelectrolytes*; Marcel Dekker: New York, 1971.
- (2) Ullner, M. In *Handbook of Polyelectrolytes and Their Applications*; Tripathy, S. K., Kumar, J., Nalwa, H. S., Eds.; American Scientific: Stevenson Ranch, CA, 2002; Vol. 3, p 271.
- (3) Wandrey, C.; Hunkeler, D. In *Handbook of Polyelectrolytes and Their Applications*; Tripathy, S. K., Kumar, J., Nalwa, H. S., Eds.; American Scientific: Stevenson Ranch, CA, 2002; Vol. 2, p 147.
- (4) Schmidt, M. E. *Polyelectrolytes with Defined Molecular Architecture II*; Springer-Verlag: Berlin, Germany, 2004.
- (5) Ulrich, S.; Laguecir, A.; Stoll, S. *Macromolecules* **2005**, *38*, 8939.
- (6) Dobrynin, A. V. *Curr. Opin. Colloid Interface Sci.* **2008**, *13*, 376.
- (7) Schwoyer, W. L. K. *Polyelectrolytes for Water and Wastewater Treatment*; CRC Press: Boca Raton, FL, 1981.
- (8) Kam, S.-K.; Gregory, J. *Water Res.* **2001**, *35*, 3557.
- (9) Hunkeler, D. *Spec. Chem. Mag.* **2003**, *23*, 21.
- (10) Berret, J.-F.; Schonbeck, N.; Gazeau, F.; El Kharrat, D.; Sandre, O.; Vacher, A.; Airiau, M. *J. Am. Chem. Soc.* **2006**, *128*, 1755.
- (11) Meijer, E. W.; Van Genderen, M. H. P. *Nature* **2003**, *426*, 128.
- (12) Allen, T. M.; Cullis, P. R. *Science (Washington, DC, U.S.)* **2004**, *303*, 1818.
- (13) Cooper, C. L.; Dubin, P. L.; Kayitmazer, A. B.; Turksen, S. *Curr. Opin. Colloid Interface Sci.* **2005**, *10*, 52.
- (14) Cooper, C. L.; Goulding, A.; Kayitmazer, A. B.; Ulrich, S.; Stoll, S.; Turksen, S.; Yusa, S.-I.; Kumar, A.; Dubin, P. L. *Biomacromolecules* **2006**, *7*, 1025.
- (15) Ullner, M.; Joansson, B.; Widmark, P. O. *J. Chem. Phys.* **1994**, *100*, 3365.
- (16) Katchalsky, A.; Spitnik, P. *J. Polym. Sci.* **1947**, *2*, 432.
- (17) Nagasawa, M.; Holtzer, A. *J. Am. Chem. Soc.* **1964**, *86*, 531.
- (18) Nagasawa, M. *Pure Appl. Chem.* **1971**, *26*, 519.
- (19) Mandel, M. *Eur. Polym. J.* **1970**, *6*, 807.
- (20) Burak, Y.; Netz, R. R. *J. Phys. Chem. B* **2004**, *108*, 4840.
- (21) Raphael, E.; Joanny, J. F. *Europhys. Lett.* **1990**, *13*, 623.
- (22) Braud, C. *Eur. Polym. J.* **1975**, *11*, 421.
- (23) Vallat, P.; Catala, J. M.; Rawiso, M.; Schossel, F. *Europhys. Lett.* **2008**, *82*, 28009/1.
- (24) Borukhov, I.; Andelman, D.; Borrega, R.; Cloitre, M.; Leibler, L.; Orland, H. *J. Phys. Chem. B* **2000**, *104*, 11027.
- (25) Kesvatera, T.; Jonsson, B.; Thulin, E.; Linse, S. *Proteins: Struct. Funct., Genet.* **1999**, *37*, 106.
- (26) Porasso, R. D.; Benegas, J. C.; van den Hoop, M. A. G. T.; Paoletti, S. *Biophys. Chem.* **2000**, *86*, 59.
- (27) Manning, G. S. *J. Chem. Phys.* **1969**, *51*, 924.
- (28) Olvera de la Cruz, M.; Belloni, L.; Delsanti, M.; Dalbiez, J. P.; Spalla, O.; Drifford, M. *J. Chem. Phys.* **1995**, *103*, 5781.
- (29) Wittmer, J.; Johner, A.; Joanny, J. F. *J. Phys. II* **1995**, *5*, 635.
- (30) Schiessel, H.; Pincus, P. *Macromolecules* **1998**, *31*, 7953.
- (31) Barbosa, M. C.; Deserno, M.; Holm, C. *Europhys. Lett.* **2000**, *52*, 80.
- (32) Deshkovski, A.; Obukhov, S.; Rubinstein, M. *Phys. Rev. Lett.* **2001**, *86*, 2341.
- (33) Muthukumar, M. *J. Chem. Phys.* **2004**, *120*, 9343.
- (34) Dobrynin, A. V. *Macromolecules* **2006**, *39*, 9519.
- (35) Gonzalez-Mozuelos, P.; Olvera de la Cruz, M. *J. Chem. Phys.* **1995**, *103*, 3145.
- (36) Solis, F. J.; Olvera de la Cruz, M. *J. Chem. Phys.* **2000**, *112*, 2030.

- (37) Solis, F. J.; Olvera de la Cruz, M. *Eur. Phys. J. E* **2001**, *4*, 143.
- (38) Kundagrami, A.; Muthukumar, M. *J. Chem. Phys.* **2008**, *128*, 244901/1.
- (39) Nguyen, T. T.; Rouzina, I.; Shklovskii, B. I. *J. Chem. Phys.* **2000**, *112*, 2562.
- (40) Reed, C. E.; Reed, W. F. *J. Chem. Phys.* **1992**, *96*, 1609.
- (41) Ullner, M.; Joensson, B. *Macromolecules* **1996**, *29*, 6645.
- (42) Ullner, M.; Woodward, C. E. *Macromolecules* **2000**, *33*, 7144.
- (43) Laguerre, A.; Ulrich, S.; Labille, J.; Fatin-Rouge, N.; Stoll, S.; Buffle, J. *Eur. Polym. J.* **2006**, *42*, 1135.
- (44) Limbach, H. J.; Holm, C. *J. Chem. Phys.* **2001**, *114*, 9674.
- (45) Zito, T.; Seidel, C. *Eur. Phys. J. E* **2002**, *8*, 339.
- (46) Khan, M. O.; Mel'nikov, S. M.; Joensson, B. *Macromolecules* **1999**, *32*, 8836.
- (47) Sarraguca, J. M. G.; Skepo, M.; Pais, A. A. C. C.; Linse, P. *J. Chem. Phys.* **2003**, *119*, 12621.
- (48) Klos, J.; Pakula, T. *J. Chem. Phys.* **2005**, *123*, 024903/1.
- (49) Hsiao, P.-Y. *Macromolecules* **2006**, *39*, 7125.
- (50) Hsiao, P.-Y.; Luijten, E. *Phys. Rev. Lett.* **2006**, *97*, 148301/1.
- (51) Stevens, M. J. *Biophys. J.* **2001**, *80*, 130.
- (52) Ou, Z.; Muthukumar, M. *J. Chem. Phys.* **2005**, *123*, 074905/1.
- (53) Wei, Y.-F.; Hsiao, P.-Y. *J. Chem. Phys.* **2007**, *127*, 064901/1.
- (54) Metropolis, N.; Rosenbluth, A. W.; Rosenbluth, M. N.; Teller, A. H.; Teller, E. *J. Chem. Phys.* **1953**, *21*, 1087.
- (55) Verdier, P. H.; Stockmayer, W. H. *J. Chem. Phys.* **1962**, *36*, 227.
- (56) Wall, F. T.; Mandel, F. *J. Chem. Phys.* **1975**, *63*, 4592.
- (57) Gordon, H. L.; Valleau, J. P. *Mol. Simul.* **1995**, *14*, 361.
- (58) Stevens, M. J.; Kremer, K. *J. Chem. Phys.* **1995**, *103*, 1669.